Available online at www.sciencedirect.com
SCIENCE DIRECT
ELSEVIER
Journal of the European Ceramic Society 26 (2006) 2979–2983
ECERS
www.elsevier.com/locate/jeurceramsoc

Synthesis of Al-doped ZnO nanomaterials with controlled luminescence

Robert R. Piticescu [a,*], Roxana M. Piticescu [a], Claude J. Monty [b]

[a] *National Research and Development Institute for Non-ferrous&Rare Metals,102 Biruintei Blvd., Pantelimon, Ilfov, Romania*
[b] *CNRS/Procédés, Matériaux et Energie Solaire (Font-Romeu), France*

Available online 10 March 2006

Abstract

Due to the combination of interesting piezoelectric, electric, optical and thermal properties ZnO-doped nanomaterials are of high interest for multifunctional applications in gas sensors, ultrasonic oscillators or transparent electrodes in solar cells. Their implementation and utilisation is strongly dependant on the microstructure and surface nanochemistry characteristics. New processes for the synthesis and sintering are required to control and optimize the chemical composition, component distribution, crystalline and grain sizes. We present the results on the synthesis of zinc oxide powders with different Al content by two different procedures: hydrothermal route and evaporation–condensation in a solar furnace.

The influence of the synthesis parameters on the chemical and microstructural characteristics of nanophases synthesized in the two methods has been systematically studied using chemical methods, XRD, BET, picnometric density, SEM and TEM. The combination of the two methods is demonstrated to be a powerful way to obtain nanomaterials with controlled composition and morphology that could not be successfully realised using classical routes. Al doping leads to a lower material density and to a smaller grain size. The first results on the luminescence properties of Al-doped ZnO nanopowders are also presented.

Keywords: ZnO; Nanoparticles

1. Introduction

Currently, ZnO presents a great interest for the scientific community due to its applications in different fields: UV light emitters, varistors, transparent high power electronics, surface acoustic wave devices, piezoelectric transducers, gas sensing and as window material for display and solar cells. The most significant impediment in developing and exploiting zinc oxide based materials in electronic and photonic applications is the difficulty in carrier doping (achieving a p-type material); n-type conductivity of ZnO is relatively easy to realize using excess Zn or by doping zinc oxide with Al, Ga, In.[1] The most promising dopants for obtaining p-type conductivity are the elements from the Vth group.

Different routes to obtain doped ZnO materials (e.g. visible light photo catalyst for solar energy and interior lighting applications) have been studied,[2] namely: the incorporation of transition metal ions (e.g. V or Cr ions) into a semiconductor photo catalyst by ion implantation or by co-precipitation; introduction of oxygen vacancies by treating a photo catalyst with hydrogen plasma or X-ray irradiation; coupling semiconductors (ZnO or TiO_2) with oxides that enable visible light absorption (WO_3, Fe_2O_3, CdS) by co-precipitation or impregnation; doping of N-atoms into the substitutional sites in the crystal structure of a photo catalyst (TiO_2 or Ta_2O_3) by calcination in an ammonia atmosphere. Li et al. applied the spray pyrolysis technique to prepare N-containing MO_x–ZnO (M = W, Fe, V) to obtain visible light photo catalyst zinc oxide based novel materials.[2]

In the science and technology of zinc oxide several key issues have to be achieved[3]: controlling the morphology and chemical composition of the zinc oxide powders; purity and particle size during the synthesis of zinc oxide powders; controlling the level of the dopants. Zinc oxide powders with different morphology (prismatic, ellipsoidal, bi-pyramidal, dumbbell-like, nanowire, nanorod) were obtained.

Thin films of zinc oxide exhibit many advantages: they can be fabricated in small dimensions in large scale, low cost production and are widely compatible with microelectronic technology and circuits. Zinc oxide films can be obtained by RF sputtering, PLD, CVD, MOPVE, molecular beam epitaxy,[4] sol–gel processes starting from zinc acetate, ammonia or alumina powders,[5] and thermal evaporation of zinc acetate.[6]

* Corresponding author. Tel.: +40 21 2552692; fax: +40 21 25574 88.
E-mail address: rpiticescu@rdslink.ro (R.R. Piticescu).

0955-2219/$ – see front matter © 2006 Elsevier Ltd. All rights reserved.
doi:10.1016/j.jeurceramsoc.2006.02.015

It is well known that the size range below 100 nm is of greatest interest for the scientific community and represents the greatest application potential. Nanoparticles can be manufactured by four generic routes: wet chemical, mechanical, form-in-place and gas phase synthesis.[7] Wet chemical procedures include: sol–gel methods, hydrothermal techniques and precipitation processes. Mechanical processes include grinding, milling and mechanical alloying techniques. Form-in-place processes include lithography, vacuum deposition techniques (CVD, PVD), spray coatings. Gas phase synthesis includes flame pyrolysis, electro-explosion, laser ablation, high temperature evaporation, plasma synthesis techniques.

A significant number of powders and films can be obtained in hydrothermal conditions at temperatures in the range 25–200 °C and pressures <1.5 MPa in conditions interesting for the industry,[8] due to advantages of versatility: it is an environmentally friendly procedure due to the fact that it takes place at limited temperatures and pressures, closely to those of living conditions on the Earth; there are low reactions temperatures (avoiding problems related to the volatilisation of components and stress induced defects); the rate and uniformity of nucleation, growth and aging can be controlled; powders, fibbers, single crystals, monolithic bodies, coatings on metals, polymers, and ceramics can be prepared; the costs for energy, instrumentation and precursors are lower. According to Yoshimura and Suchanek[9] a large quantity of energy is necessary to create melt, vapour, gas, plasma compared to the formation of an aqueous solution at the same temperature. The time and energy consumption is lower for the hydrothermal processes due to the fact that mixing and milling steps are not necessary.

This paper deals with Al-doped ZnO nanopowders synthesised by hydrothermal route and processed in a solar reactor to increase the microstructural quality and decrease the size of the nanophases. The aim of this work was to establish the influence of the synthesis parameters on the chemical and microstructural characteristics of the Al-doped ZnO nanophases and to study their influence on the luminescence properties.

2. Experimental procedure

The hydrothermal synthesis of alumina doped zinc oxide nanopowders was performed in a 2L computer-controlled Teflon autoclave (CORTEST, USA) using KOH as a mineralising agent. The precipitates were filtered, washed with distilled water to remove the soluble chlorides and ethanol to reduce agglomeration and dried for several hours in air at 110 °C.

Al-doped ZnO nanophase particles have been prepared by the vaporization–condensation method starting from Al-doped zinc oxide synthesised in hydrothermal conditions in a solar reactor consisting of a glass balloon placed at the focus of a solar PVD furnace. The material is sublimated inside the evaporation chamber by using solar heating power, focused on the sample by means of a parabolic mirror. The vapours are condensed as a smoke which is collected on a cold finger or/and on a metallic filter under vacuum. One other advantage of this process is that it can remove volatile impurities such as the smallest traces of nitrides or chlorides that could be present in the powder even after washing.

The powders composition was determined by chemical quantitative analysis using inductively coupled plasma–ICP (SPECTROFLAME Germany); direct coupled plasma–DCP (SPECTRASPAN V/Beckman/USA), atomic absorption spectrometry–AAS (AAS 30 Karl Zeiss Jena), colorimetric methods (SPECORD M 40).

Powder phase analysis was investigated by X-ray diffraction analysis using a Phillips Analytical X-ray RV type PW 3710700. Commercial yttria powder was used an internal reference to calibrate the position of the peaks for Al-doped ZnO nanopowders. Commercial ZnO powder was annealed in the furnace at 900 °C, in air for 48 h; the annealed powder thus obtained was used to calculate the instrumental width of the diffraction ray. The mean crystallite sizes were determined using PROFIT programme of the Diffractometer. The fundamental equation to determine the size of a crystallite at the intrinsic width of the diffraction ray was the usual Scherrer equation:

$$d_{\mathrm{m}} = \frac{k\lambda}{\delta \cos\theta} \tag{1}$$

where d_{m} is the mean crystallite size, k the constant which depend on the shape of the crystallite, Miller indexes and Bragg demonstrated that its value is near 0.9, θ the Bragg diffraction angle, λ the wave length of the incident radiation, δ the intrinsic width of the diffraction ray.

BET specific surface area of powders was determined on a Gemini 2360—Micromeritics Instruments apparatus. Picnometric density was determined using and Acupyc apparatus. The equivalent mean grain sizes (in nm) were calculated from:

$$d_{\mathrm{m}} = \frac{6}{S\rho} \times 1000, \tag{2}$$

where S is the specific BET surface area (in m^2/g) and ρ the picnometric density (in g/cm^3) of nanopowders.

Powder morphology was analyzed by scanning electron microscopy (SEM, Gemini LEO 1530) and for selected powders by TEM.

Luminescence spectra of powders doped with Al obtained by hydrothermal method and solar PVD method having different Al dopant levels were measured using a Nd:YAG laser source generating the second harmonic wave length at 532 nm.

Table 1
Chemical composition of initial powders

Sample	Chemical analysis (weight %)		Composition (at.%)		
	Al	Ignition loss at 1000 °C	Al	Zn	O
0.05 AlZnO initial	0.026	1.65	0.040	50.489	49.471
0.1 AlZnO initial	0.053	1.05	0.081	50.272	49.647
0.25 AlZnO initial	0.14	1.37	0.215	50.281	49.504
0.5 AlZnO initial	0.45	1.81	0.693	50.090	49.217
ZnO_4 Al initial	0.95	2.05	1.461	49.637	48.902

All samples were obtained at 250 °C, 30 min at high alkaline pH

Table 2
Chemical composition of solar PVD nanophases

Sample	Working conditions		Chemical analysis (weight %)		Composition (at.%)		
	Solar flux (W/m^2)	Pressure (Torr)	Al	Ignition loss at 1000 °C	Al	Zn	O
0.05ALZnO-vc3	960	125	0.025	2.29	0.039	50.692	49.269
0.25ALZnO-vc8	700	50	0.14	1.86	0.216	50.434	49.350
0.5AlZnO-vc9	473	50	0.15	3.15	0.236	50.829	48.935
ZnO4Al-vc1F	965	40	0.019	0.82	0.029	50.236	49.735
ZnO4Al-vc4F	850	20	0.02	1.26	0.031	50.373	49.596

Table 3
BET analysis, density and grain size determinations for Al-doped ZnO powders

Crt. no.	Composition (mol% Al)	BET (m^2/g)	Density (g/cm^3)	Average grain size (nm)
1[a]	0.1	9.3879	5.3932	119
2	0.1	22.3151	5.6718	47
3[a]	0.5	17.155	5.3175	88
4	(0.5)/0.236	22.2015	5.5455	66
5[a]	0.25	12.8575	5.3083	49
6	(1)/0.029	37.6204	4.7774	33

[a] Samples 1, 3 and 5 were as prepared powders by hydrothermal treatment. The other samples were subjected to vaporization–condensation in the solar reactor (values in parenthesis are for starting powders).

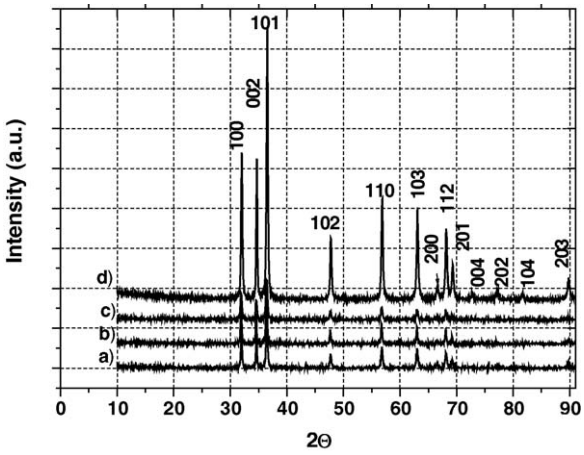

Fig. 1. XRD spectra for Al-doped ZnO nanopowders: (a) 0.1 mol% Al–ZnO hydrothermal; (b) 0.1 mol% Al–ZnO vapour-condensed; (c) 0.5 mol% Al–ZnO hydrothermal; (d) 0.5 mol% Al–ZnO vapour-condensed.

3. Results and discussion

The chemical compositions for different alumina doped zinc oxide nanopowders synthesised in hydrothermal conditions are presented in Table 1. The chemical composition of the nanophase materials after vaporisation–condensation of the initial hydrothermal powders in the solar PVD furnace at different partial pressures and solar flux are presented in Table 2. It can be observed that the level of Al in the solar PVD nanophases has a maximum threshold around 0.24 at.% Al due to the lower partial pressure of Al_2O_3 compared to ZnO. It is nevertheless important to note that in experiments made on powders with similar Al content obtained by mechanical mixing in high energy ball

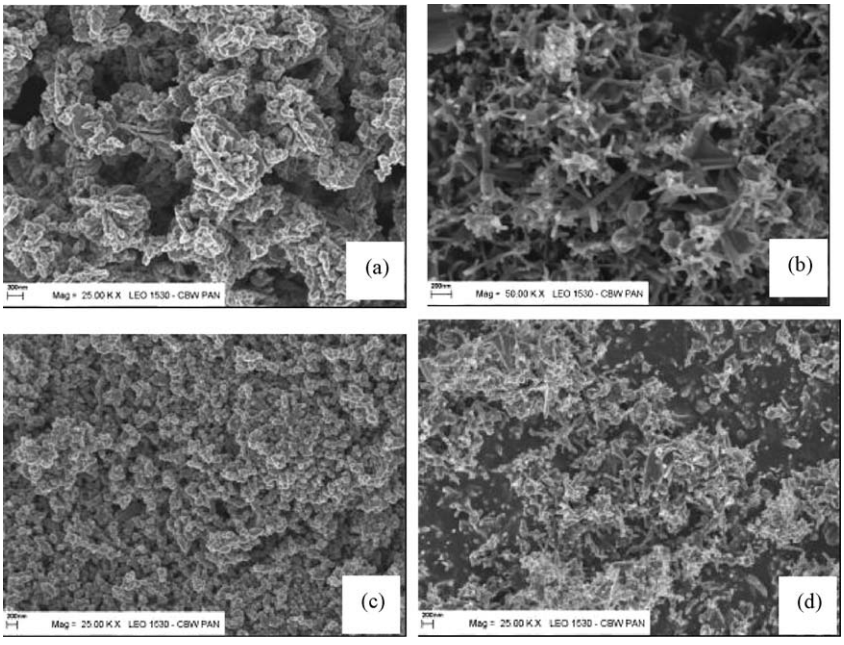

Fig. 2. Scanning electron microscopy images for different Al-doped zinc oxide samples: (a) 0.1AlZnO hydrothermal conditions; (b) 0.1AlZnO vc5-solar PVD; (c) 0.5 AlZnO hydrothermal conditions; (d) 0.5AlZnO vc9-solar PVD.

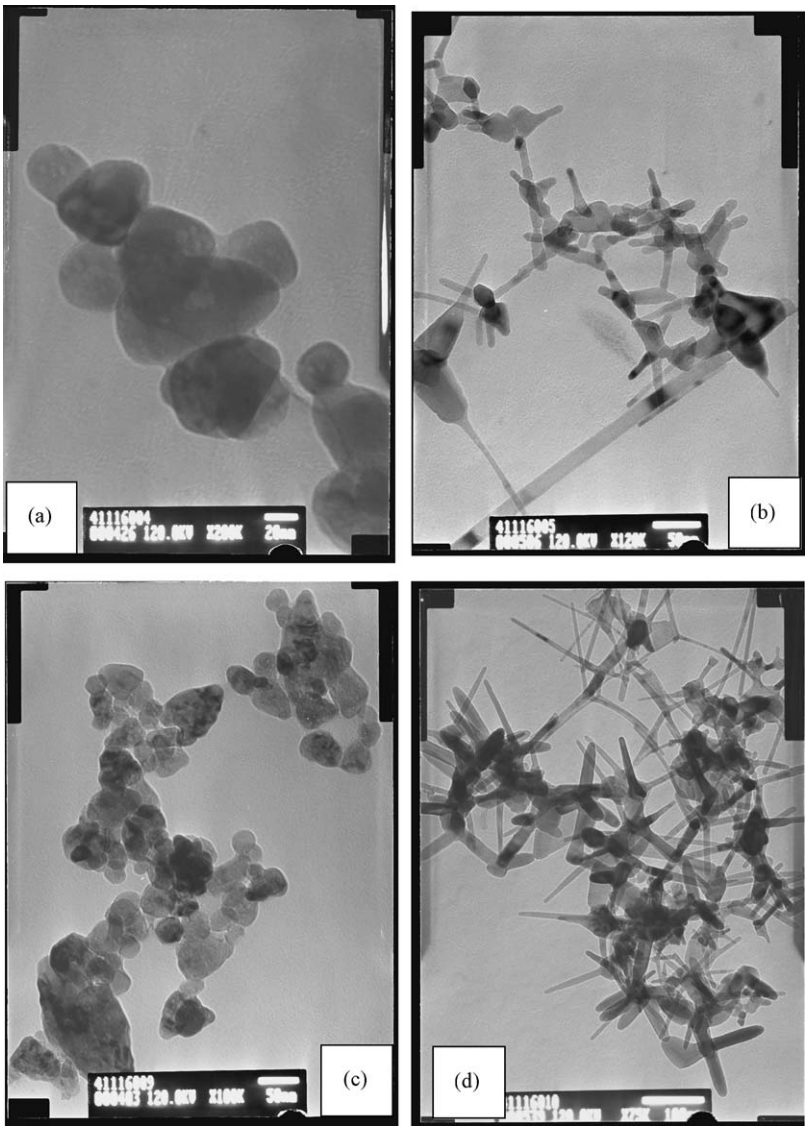

Fig. 3. Transmission electron microscopy images for different Al-doped zinc oxide samples: (a) 0.1AlZnO hydrothermal conditions; (b) 0.1AlZnO vc5-solar PVD; (c) 0.5 AlZnO hydrothermal conditions; (d) 0.5AlZnO vc9-solar PVD.

milling the amount of Al detected in solar PVD nanophases was practically zero. The results obtained after BET analysis and picnometric density measurements on some samples are presented in Table 3.

X-ray diffraction phase analysis (Fig. 1) showed that all the samples, independent of alumina content, present only the corresponding zinc oxide peaks (according to JCPDS 80-0075). As in the case of some other ceramic powders, hydrothermal synthesis leads to nanostructured powders. As expected, both BET analysis and grain size determinations (XRD) indicate a finer powder after the vaporization–condensation process. From Table 3 it can be seen that the larger the aluminium content the smaller the grain size.

The formation of double oxide gahnite ($ZnO{\cdot}Al_2O_3$) could only be observed in the initial powders with over 10 at.% A; its disappearance after vaporisation–condensation may be related to the variation of the dopant concentration after this processing. Some results from the microstructure analysis by SEM and TEM are presented in Figs. 2 and 3. Scanning electron microscope analysis for the powders synthesised under hydrothermal conditions (Fig. 2a and c) show the influence of the aluminium dopant content on the nanopowders morphology and grain size. With increasing aluminium content the morphology changes from flower like to spherical shape with a homogeneous distribution of the grain sizes. Scanning electron microscopy of Al zinc oxide powders after solar PVD processing of hydrothermal powders (Fig. 2b and d) demonstrates a lower grain size compared that for the hydrothermal powders and the formation of zinc oxide whiskers.

The TEM investigation of the powders synthesised under hydrothermal conditions showed the existence of the nanocrystalline structures with spherical morphology. Fig. 3a and c show nanoparticles linked in branch-like chains. The TEM investigation of the vapour-condensed powders (Fig. 3b and d) displays a different morphology; the particles have a whiskers shape. The evolution of luminescence spectra for the same powders is pre-

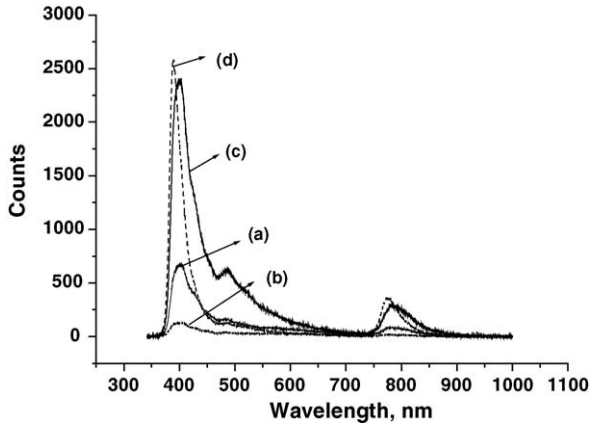

Fig. 4. Luminescence spectra for hydrothermal and vapour-condensed powders: (a) 0.1 mol% Al–ZnO hydrothermal; (b) 0.1 mol% Al–ZnO vapour-condensed; (c) 0.5 mol% Al–ZnO hydrothermal; (d) 0.5 mol% Al–ZnO vapour-condensed.

sented in Fig. 4. The small shoulder at ≈500 nm corresponds to pure ZnO. With increasing Al level in the initial powders the peak intensity increases and there is a slight shift of the peaks. However, there is no important modification for nanopowders obtained via hydrothermal or solar-PVD processes. The first band has been attributed to free excitons and the second band to bound excitons.

4. Conclusions

Hydrothermal synthesis was used for the preparation of nanostructured Al-doped ZnO nanopowders with controlled Al content. The grain morphology for this material can be changed by subjecting the powders to a vaporization–condensation process in a solar reactor under controlled flux and pressure. The agglomerated nanograins of the hydrothermal powders have different shapes depending on the Al content; the vapo-condensed powders are formed as nanowhiskers, as shown by SEM and TEM microstructural analysis. A loss of Al dopant takes place during this process which could be responsible for increase in density. The combination of the two methods is hence a powerful way to obtain nanomaterials with controlled composition and morphology that could not be successfully realised using classical routes.

Al doping leads to a lower material density and to a smaller grain size—the bigger the aluminium content the finer the grain size and, of course, the higher specific surface. The double oxide $ZnAl_2O_4$ in the hydrothermal synthesised powders with high Al content (over 10 at.%) is not present in the solar PVD material due to the lower Al content.

Luminescence spectra show enhanced intensity with increasing Al doping. The combined role of Al and grain size effects on luminescence spectra are under study using fine peak profile analysis and grain size distribution perpendicularly and along the whiskers for vapour condensed powders.

Acknowledgements

The authors are indebted to the SOLFACE European project and ECO-NET Project “Fun-Nanos” managed by EGIDE, France, which provided support for experiments at the Solar Facilities of the PROMES laboratory in Font Romeu (France).

The authors thank Ph.D. student Tomasz Strachowski and Dr. Adam Presz from Institute of High Pressure Physics, Warsaw, Poland for their work on solar PVD and microstructural characterization respectively. TEM figures have been done by Hubert Matysiak from Faculty of Materials Science of Warsaw University of Technology.

References

1. Pearton, S. J., Norton, D. P., Ip, K., Heo, Y. W. and Steiner, T., *Superlattices Microstruct.*, 2003, **34**, 3–32.
2. Li, Di. *et al.*, *Catal. Today*, 2004, **93–95**, 895–901.
3. Xu, H. Y. *et al.*, *Ceram. Int.*, 2004, **30**, 93–97.
4. Zhaochun, Z. *et al.*, *Mat. Sci. Eng.*, 2001, **B86**, 109–112.
5. Cai, K. F. *et al.*, *Mater. Sci. Eng.*, 2003, **B 104**, 45–48.
6. Jin, M. *et al.*, *Thin solid films*, 1999, **357**, 98–101.
7. Pitkethy, M. J., *Nanotoday*, 2004.
8. Riman, R. E., *Ann. Chim. Sci. Mat.*, 2002, **27**(6), 16–36.
9. Yoshimura, M. and Suchanek, W., *Solid State Ionics*, 1997, **98**, 197–208.